Experimental Observations of Wall Interference at Transonic Speeds

R. F. Starr*
ARO, Inc., Arnold Air Force Station, Tenn.

Lift and downwash interference on the high-aspect-ratio ONERA calibration configuration have been isolated from other variables (such as tunnel flow quality, "effective" Reynolds number, and model distortion under load) which are present in comparative wind tunnel data. The lift interference on the ONERA configuration was found to be related to the model to tunnel span ratio and is highly nonlinear in normal force at transonic speeds. Fighter and lifting body configurations were also studied. These lower aspect ratio configurations ($AR<4$) were found to be much less sensitive to wall interference. A family of curves which can be used to estimate lift and pitching-moment interference at transonic speeds is presented, and an empirical dependency of lift interference on AR^2 is suggested.

Nomenclature

AR = aspect ratio $= b^2/S$
b = model span, ft
C_{AF} = forebody axial-force coefficient = forebody axial force$/q_\infty S$
C_m = pitching-moment coefficient = pitching moment$/q_\infty S\bar{c}$
C_N = normal-force coefficient = normal force$/q_\infty S$
C_n = local normal-force coefficient determined from pressure distribution at one wing station
C_p = wing pressure coefficient $= (p-p_\infty)/q_\infty$
$C_p{}^*$ = wing pressure coefficient for sonic flow $= (p^*-p_\infty)/q_\infty$
c = local chord
$\bar{c}$ = mean aerodynamic chord
D_F = fuselage diameter
L_F = fuselage length
M_∞ = freestream Mach number
p = local pressure
p_∞ = freestream pressure
q_∞ = freestream dynamic pressure
$Re_{\bar{c}}$ = Reynolds number based on mean aerodynamic chord
S = model reference area, ft^2
$\bar{X}$ = distance from moment reference center to leading edge of horizontal tails, ft
X/c = nondimensional distance from wing leading edge
Y = horizontal distance from the tunnel centerline
Z = vertical distance from the tunnel centerline
α = model angle of attack determined by gravimetric sensor in model fuselage
α_d = increment in downwash angle at the horizontal tail
α_u = increment in upwash angle at wing station 2
α_w = angle of attack at wing station 2 determined from pressure difference at two orifices on wing nose
ΔC_m = increment in pitching-moment coefficient attributed to wall interference
ΔC_N = increment in normal-force coefficient attributed to wall interference
τ_w = tunnel wall porosity

Presented as Paper 78-164 at the AIAA 16th Aerospace Sciences Meeting, Huntsville, Ala., Jan 16-18; submitted Jan. 18, 1978; revision received June 23, 1978.

Index categories: Aerodynamics; Testing, Flight and Ground; Transonic Flow.

*Engineering Supervisor, 4T Projects Branch, AEDC Division. Member AIAA.

Introduction

THE influence of the tunnel boundary on the aerodynamic simulation achieved in wind tunnels has been extensively studied since the early days of wind tunnel testing. However, concrete information on wall interference at transonic speeds for practical aerodynamic configurations has been difficult to obtain. To experimentally evaluate wall interference, the model size or tunnel size or both are usually changed. Unfortunately, the relative influence of the tunnel wall is not the only parameter which is changed in a comparison of this type. The spatial distribution of the flow, the effective Reynolds number, the relative aeroelastic distortion, and in some cases, the model support geometry are also altered. Increments in the measured data obtained at transonic speeds cannot be easily attributed to any one of the four variables,[1] since all are relatively second-order terms of comparable magnitude and effect.

It is convenient to quantify the spatial distribution of the flow which exists in all wind tunnels, in terms of a cross-sectional flow angle distribution at transonic speeds. Such a distribution is given in Fig. 1 for a typical transonic tunnel. If the model is altered or the comparison is conducted in two different tunnels, differential flow quality effects can be introduced into the aerodynamic data obtained.

With regard to Reynolds number, the transition Re is known to vary with unit Re within a given tunnel[2,3] and from

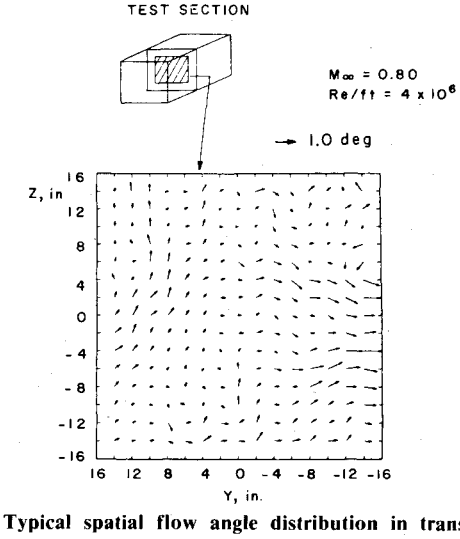

Fig. 1 Typical spatial flow angle distribution in transonic wind tunnel.

tunnel to tunnel for a fixed unit *Re*. Transonic flow is especially sensitive to Reynolds number, since the viscid and inviscid flowfields are often strongly coupled. Maintaining a fixed "effective" Reynolds number (transition *Re* and chord *Re*) involves fixing transition and controlling the state of the boundary layer over the body for a valid wall interference comparison. Such a fix in "effective" *Re* is difficult to achieve in transonic flow, especially when the model size is altered significantly. Most high-aspect-ratio wing models are also relatively flexible even for wind tunnel loadings. The aeroelastic shape of the wing changes slightly but significantly with aerodynamic load, which is related to total pressure or Reynolds number and can appear as an erroneous *Re* effect.

Finally, practical mechanical considerations may necessitate some relative change in model support geometry when either the model size or the tunnel is changed.

Three comparative tests have recently been conducted at the Arnold Engineering Development Center in the 4-ft × 4-ft aerodynamic wind tunnel (4T) and the 16-ft × 16-ft propulsion wind tunnel (16T). A lifting body configuration, a fighter configuration†, and a transport configuration (ONERA calibration body[1]) were evaluated. Dimensional details of the three configurations are given in Fig. 2. Measurable wall intereference was found to be dependent on model size and aerodynamic configuration, as will be shown.

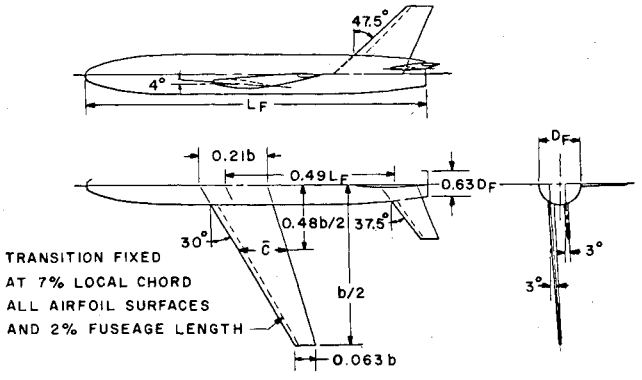

MODEL	M3	M5
WING SPAN, b, ft	1.52	3.15
FUSELAGE LENGTH, L_F, ft	1.64	3.47
REF. AREA, S, ft^2	0.32	1.36
FUSELAGE DIAMETER, D_F	0.197	0.407
MEAN AERO CHORD, c̄	0.217	0.449
ASPECT RATIO, AR	7.310	7.310
16T BLOCKAGE, %	0.018	0.077
4T BLOCKAGE, %	0.290	1.230

Fig. 2a Geometry of the ONERA M-3 and M-5 calibration bodies.

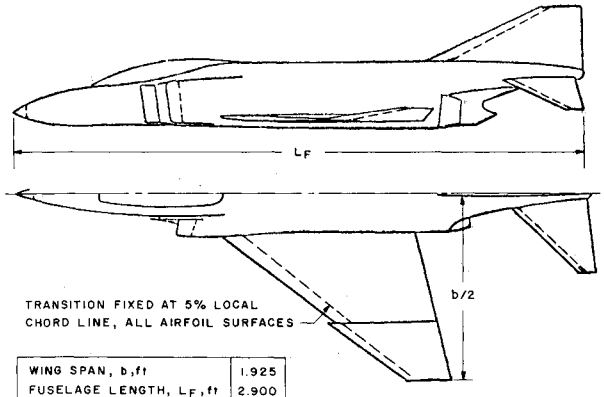

WING SPAN, b, ft	1.925
FUSELAGE LENGTH, L_F, ft	2.900
REF. AREA, S, ft^2	1.325
MEAN AERO CHORD, c̄	0.802
ASPECT RATIO, AR	2.800
16T BLOCKAGE, %	0.041
4T BLOCKAGE, %	0.660

Fig. 2b Geometric details of the fighter configuration.

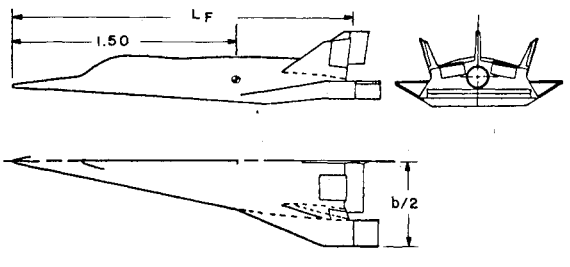

WING SPAN, b, ft	1.15
FUSELAGE LENGTH, L_F, ft	2.30
REF. AREA, S, ft^2	1.29
ASPECT RATIO, AR	1.03
16T BLOCKAGE, %	0.08
4T BLOCKAGE, %	1.37

DIMENSIONS IN FEET

Fig. 2c Geometric details of the lifting body configuration.

ONERA Configuration

Two sizes of the ONERA calibration configuration were tested in tunnels 4T and 16T, and the results were summarized in Ref. 1. Six-component force data and wing pressure distributions were obtained on the larger model (M-5) whereas force data alone were obtained on the smaller model (M-3), which is about one half the size of the larger model. An analysis of the data reveals that the angle of incidence of the mid-semispan increased about 0.4 deg relative to the fuselage for a threefold increase in *Re* (2 to 6×10^6/ft) for the larger M-5 model. The angle of incidence of the wingtip is even more sensitive to changes in aerodynamic load. In the following analysis of the ONERA configuration, only data obtained with fixed transition and at a fixed unit *Re* will be compared between the tunnels to minimize the possibility of both uncontrolled *Re* effects and variations in model aeroelastic shape due to aerodynamic load changes. Data comparisons between the two models were avoided for similar reasons.

Normal Force

The difference in normal force measured in 4T and 16T on the two models is given in Fig. 3 for fixed transition and a fixed unit *Re*. As Mach number and angle of attack are in-

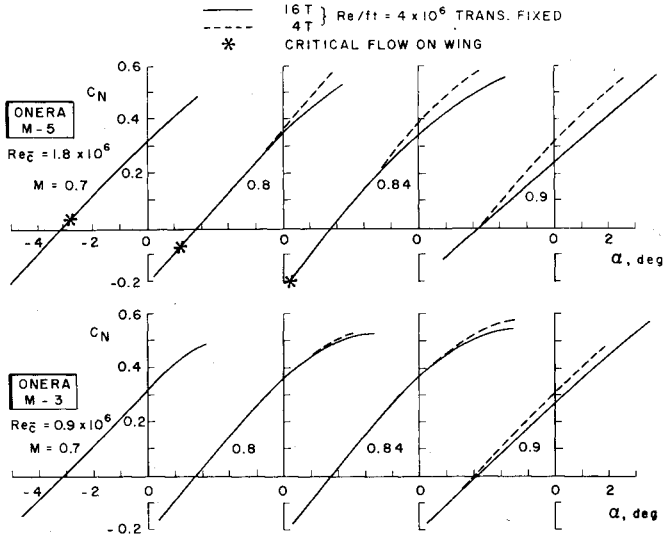

Fig. 3 Normal-force difference between the 4- and 16-ft tunnels for two ONERA model sizes at transonic speeds.

†Whoric, J.M. and Herron, R.D., 4T Projects Branch, PWT, Arnold Air Force Station, Tenn.

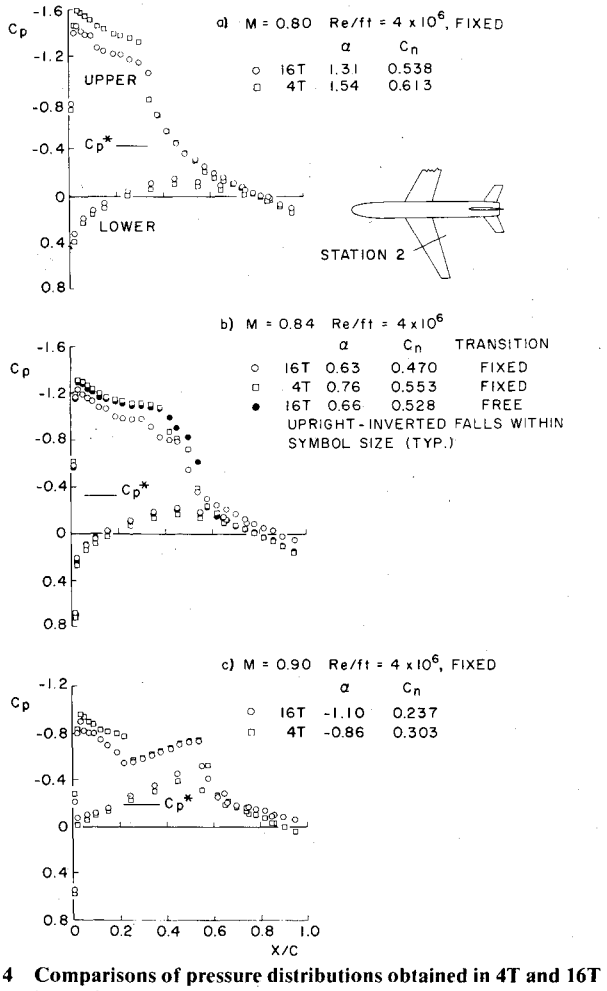

Fig. 4 Comparisons of pressure distributions obtained in 4T and 16T at the mid-semispan of the ONERA M-5.

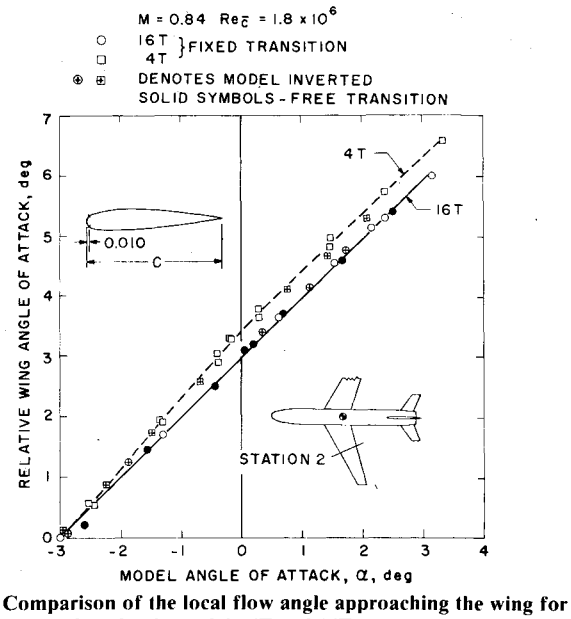

Fig. 5 Comparison of the local flow angle approaching the wing for a range of model angle of attack in 4T and 16T.

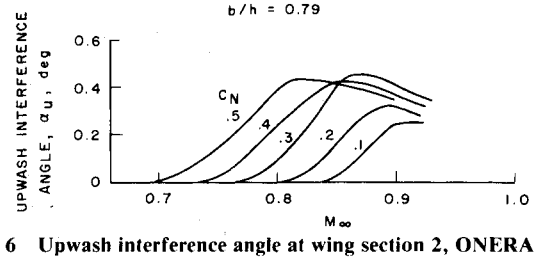

Fig. 6 Upwash interference angle at wing section 2, ONERA M-5 in 4T (relative to 16T).

creased, the results from the two tunnels digress significantly. The tunnel-to-tunnel difference is greater for the larger model at a given Mach number-angle combination than for the smaller model.

The pressure distribution at the mid-semispan is given for three Mach numbers in Fig. 4. A significant difference between 4T and 16T is seen to exist over both the upper and lower wing surfaces. These pressure differences are larger than would be expected for the relatively minor angle of attack difference noted. Supersonic flow develops on the wing at angles of attack just above those denoted by the asterisk in Fig. 3, and the supercritical region is extensive at the angles at which the tunnel-to-tunnel differences begin to appear.

The pressure difference between an upper and lower surface pressure orifice near the leading edge of the wing was used to provide a measure of the local angle of attack of the flow approaching wing station 2. In Fig. 5, the angle of the flow approaching the wing is shown to be generally greater in 4T than in 16T for a given model angle of attack. The normal-force coefficient is greater in 4T (Figs. 3 and 4), and the induced angle of attack is greater in 4T (Fig. 5).

Some uncontrolled tunnel-to-tunnel flow quality or Reynolds number phenomenon might be considered as the source of the differences. Typical data for the model in an upright position (roll zero) and inverted (roll 180) are given in Fig. 5. The upright-inverted comparison represents a measure of the effect of flow nonuniformity in a given tunnel. This difference is seen to be a small portion of the overall tunnel-to-tunnel difference and implies that flow quality variations are not a likely source of the discrepancy.

The possibility that *Re* phenomena actually account for the tunnel-to-tunnel differences must be carefully examined since transition location, turbulence level, grit application, and other parameters which contribute to the "effective" *Re* vary significantly in the data obtained from the two tunnels. The effective *Re* was varied during the test by changing the unit *Re* (*Re*/ft), which also changes transition *Re* and noise or flow turbulence level, or by removing the transition fixing strips. Producing an effective *Re* change by removing the transition fixing strips has the following advantages in isolating the variables: 1) the flow uniformity is not altered since the tunnel flow pressure level is not varied; and 2) the aeroelastic model shape is not altered by the significant model load variations with unit *Re*. For high-aspect-ratio transport configurations, both items are especially significant when small angular changes due to wall interference are sought.

As shown in Fig. 4b, the upper surface pressure distribution changed and the lift increased as the effective *Re* was reduced in 16T by changes in the location of transition; however, the lower surface pressure and induced angle of attack (Fig. 5) remained unchanged. From this analysis of the pressure distribution and the induced angle, it appears that the source of the tunnel-to-tunnel difference given in Fig. 3 is not a flow quality effect or an effective *Re* change but a wall interference phenomenon which produces a change in lift by altering the induced angle of attack and changing the pressure distribution over both the upper and lower wing surfaces. It further appears implicit in the results that the section lift and induced angle of attack are not linearly related for those conditions with supercritical flow present on the wing.

The induced angle difference, referred to as an upwash interference angle α_u can be established from data similar to that given in Fig. 5 and is given as a function of Mach number and normal force in Fig. 6 for the larger ONERA model at wing station 2. It can be seen that the upwash interference angle is highly nonlinear in Mach number and normal force.

This induced angle difference or upwash interference at one wing station does not reflect the total change in normal force

which results from the presence of wall interference, however, because the section lift and induced angle are not linearly related when supercritical flow is present on the wing and because the sectional lift characteristics vary with span. The increment in the total model force ΔC_N, which is taken from Fig. 3, is given in Fig. 7 for both ONERA models and is probably more indicative of overall interference effects. Changes in normal force of 10-20% can be attributed to the wall interference, depending on the model to tunnel size ratio, Mach number, and normal force. Again, the increment in total model force caused by interference is highly nonlinear in Mach number and normal force when supercritical flow is present on the wing. Additional observations of wall interference obtained on the ONERA configuration in the NAE 5-ft wind tunnel are presented in Ref. 4.

The interference information given in Fig. 7 appears to be closely related to the model to tunnel size ratio. That is, the small model exhibits about one half the interference of the larger model for the same Mach number and normal-force coefficient, and the small model is one half the span of the larger model. It does not appear that the normal-force increment is proportional to the square of the model span to tunnel height ratio (b^2/h^2), as classical subsonic theory would imply. For this ONERA configuration, then, the normal-force interference from both models from Fig. 7 can be approximately correlated using the parameter $C_N b/h$, as is shown in Fig. 8. The solid lines represent generalized fairings of the results. These increments can be used to provide a measure of the lift interference on a high-aspect-ratio transport configuration at transonic Mach numbers for a range of the parameter $C_N b/h$.

For general planning purposes, it appears that the model to tunnel span ratio b/h should be small, possibly less than 0.2 for reduced lift interference at transonic speeds for a transport configuration at a typical cruise C_N. On the basis of these criteria, even the data obtained in 16T would appear to be slightly in error for $M \geq 0.9$ and $C_N \sim 0.5$. Vaucheret et al.[5] and Poisson-Quinton et al.[6] confirm the validity of Fig. 8 in their study of all the ONERA model data obtained in several free-world tunnels. Vaucheret states that "the major tunnel-to-tunnel discrepancies at transonic speeds are considerably reduced if one considers only the data obtained for $b/h \leq 0.2$."[5]

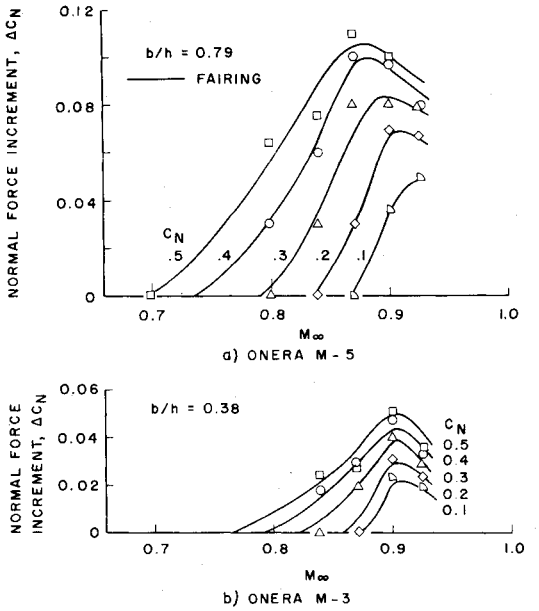

Fig. 7 Interference increment in normal force for the two ONERA models in 4T at transonic speeds (relative to 16T).

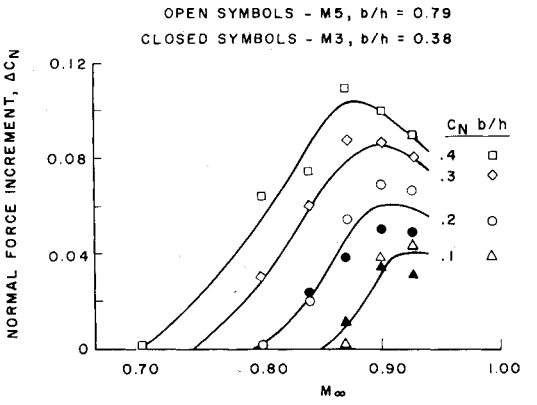

Fig. 8 Interference increment in normal force for the ONERA configuration in 4T (relative to 16T).

Pitching Moment

Significant reductions in pitching moment were also detected in the ONERA data obtained in the 4-ft tunnel and are attributed to wall interference. These differences occurred at a lower Mach number-angle combination than the normal-force differences previously presented in Fig. 3 as is shown in Fig. 9. It is difficult to quantize these differences in pitching moment in terms of an angle change at the tail or downwash interference, since the pitching-moment contribution of the wing is significant. However, if the normal-force coefficient slope of the tail is approximately equal to the wing normal-force coefficient slope, an approximate downwash interference angle at the tail can be extracted from the measured moment coefficient increments. The increment in downwash angle at the tail is given in Fig. 10 for a range of values of the classical downwash interference parameter, $\bar{X} C_N S/h^3$.

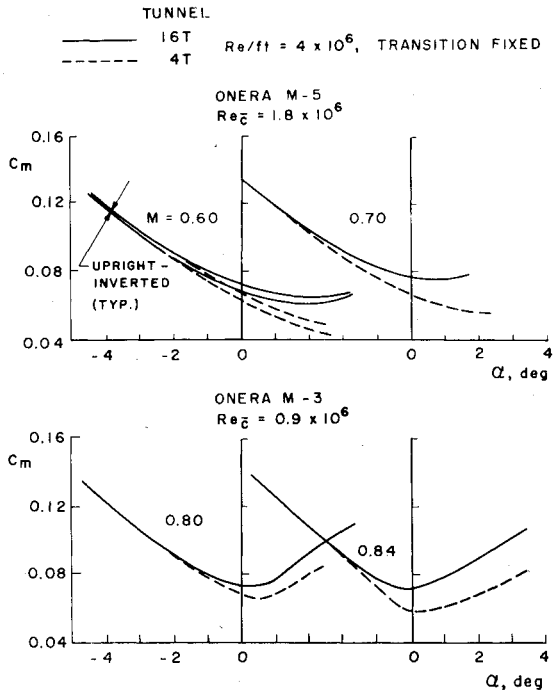

Fig. 9 Pitching-moment differences between the 4- and 16-ft tunnels for the two ONERA models at transonic speeds.

Wall Porosity Effect

The wall porosity in 4T was varied uniformly on all four walls from the usual setting of 5% open to a more closed setting of 3% and to a more open setting of 7%. The effect of porosity was found to be smaller than the 4T-16T difference in normal force or pitching moment at all Mach numbers, as shown in Fig. 11. A uniform porosity of 7% is too small from a lift interference standpoint in 4T; a differential porosity adjustment (more open top wall, more closed bottom wall) will probably be required to alleviate this interference.

Axial Force

The variation in axial force with Mach number for the ONERA configuration is given in Fig. 12. Wall interference appears in the data at about the same Mach-number/angle-of-attack combination as previously presented for normal force. It can be seen that the wall interference acts to delay the drag rise and reduce the drag at any given Mach number which is consistent with the trends in Ref. 7. The phenomena occur at progressively lower Mach numbers as normal-force increases. A uniform adjustment of wall porosity had a more pronounced effect on drag. The drag discrepancy was significantly reduced by changing the wall porosity to 3% in Tunnel 4T.

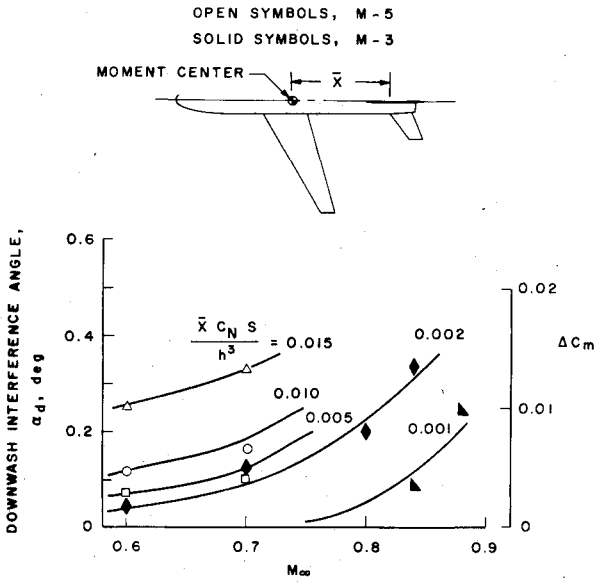

Fig. 10 Downwash interference angle on the ONERA M-3 and M-5 in 4T.

Other Configurations

Normal-force and pitching-moment variations with angle of attack are given for several transonic Mach numbers in Figs. 13 and 14 for the lifting body and the fighter configuration. Almost no measurable difference can be detected between the 4T and 16T results in either case, in spite of the rather significant relative model size in 4T (Fig. 2). The lifting surface areas for these two models are nearly the same as that of the larger ONERA model, and the total lift generated in the tunnel is nearly the same in all three cases, but few if any measurable lift or pitching-moment discrepancies were detected for these latter configurations except at $0.95 < M_\infty < 1.05$. The data were obtained with transition fixed for the fighter and with free transition for the lifting body.

The nature of the flow over the configuration, or the sectional lift characteristics, and the aspect ratio of the configuration appear to strongly influence the degree of lift interference. The high-aspect-ratio transport configuration with a "peaky" airfoil and extensive regions of supercritical flow appears to be more sensitive to small changes in streamline curvature which result from wall interference. Other airfoil shapes, with less acceleration on the suction side or a more stable shock location should be relatively less sensitive to the influence of the wall on the external flowfield. A more slender configuration, which develops less supercritical flow for a given Mach number and normal force, should also exhibit less wall interference.

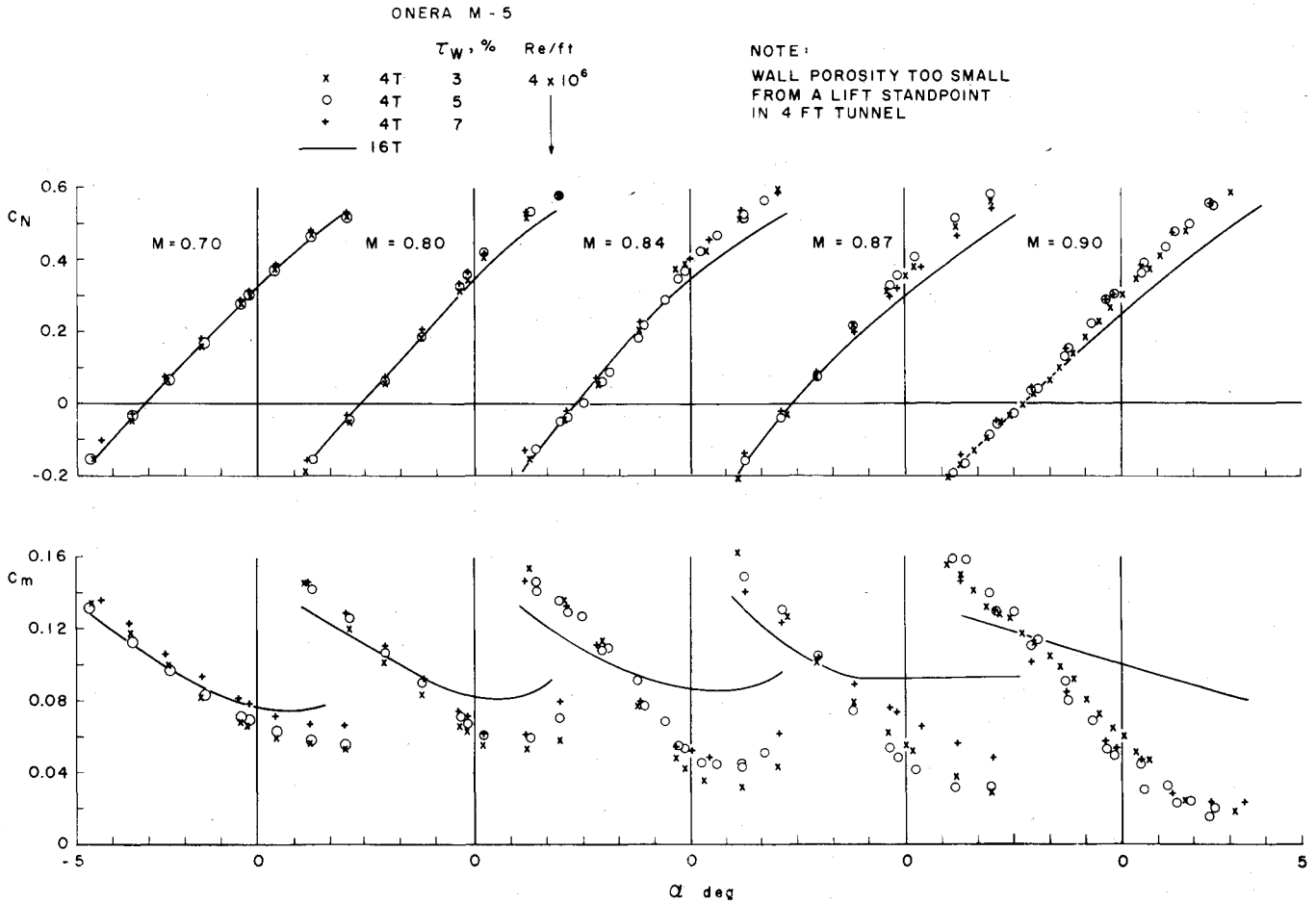

Fig. 11 Effect of wall porosity variation on normal-force and pitching-moment differences, 4T-16T.

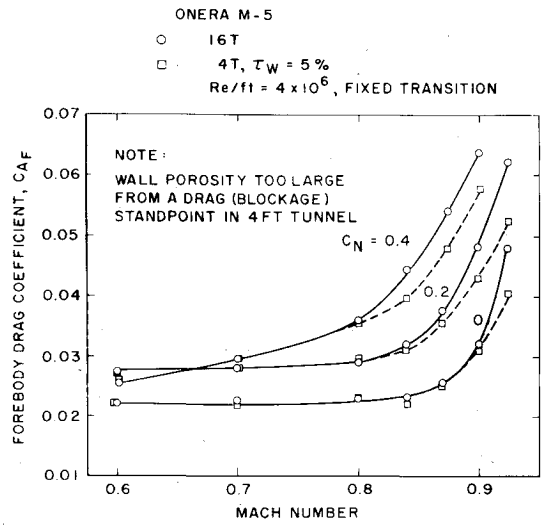

Fig. 12 Axial-force variation with Mach number.

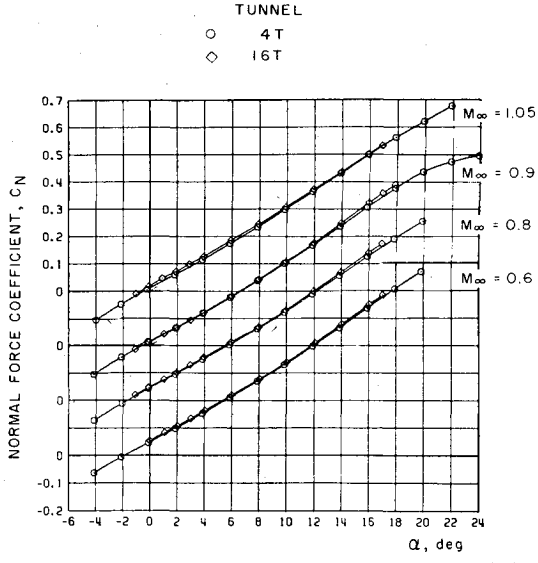

Fig. 13 Comparison of the normal force obtained on a lifting body configuration in 4T and 16T at transonic speeds.

It can be hypothesized that the aspect ratio of the configuration may play a role in the sensitivity to wall interference. For a high aspect ratio, the lift is concentrated over a relatively short portion of the tunnel length. Not only is the lift per unit length significantly different for various aspect ratios, but the opportunity for alleviation of the blockage through lateral streamline adjustment is also much greater for the low-aspect-ratio wing of a given lift (C_N and S).

If aspect ratio is appropriate, a term of the order $\mathcal{R}^2$ is required to correlate the observations on these three configurations (transport, fighter, lifting body). In rough terms, a dependency on $\mathcal{R}^2$ may reasonably account for the differing nature of the vehicle flowfields and the opportunity for lateral alleviation of the flow.

A family of curves of transonic lift interference is derived from Fig. 8 and given in Fig. 15 for the modified or empirical lift interference parameter, $C_N b/h\,\mathcal{R}^2$. Existing subsonic lift interference theory indicates a somewhat stronger influence of span ratio (b^2/h^2), as previously mentioned, and a much weaker dependence on aspect ratio than this empirical parameter.[8] The results obtained on all of the configurations discussed in this paper ($1 \leq \mathcal{R} < 8$) are consistent with the trends and magnitudes of the curves of Fig. 15, which are presented only to provide an approximate empirical indication of wall interference for a general class of bodies.

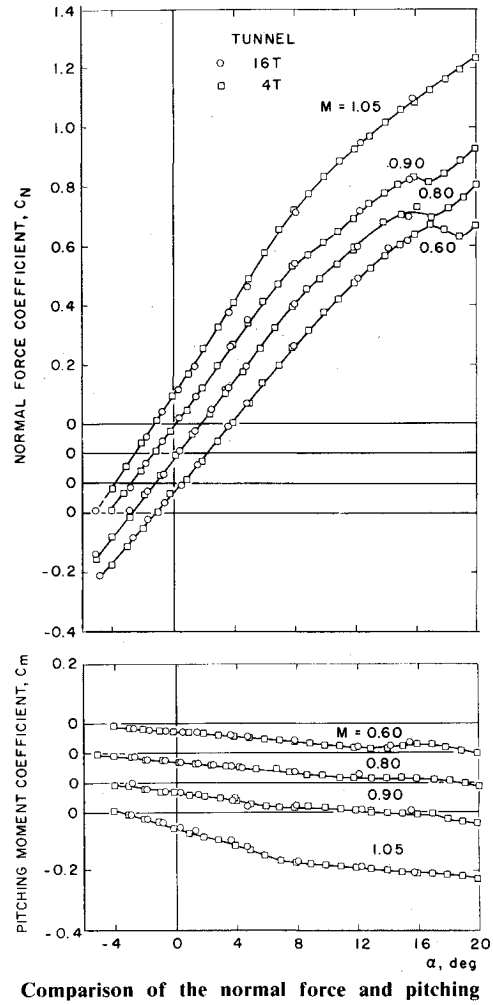

Fig. 14 Comparison of the normal force and pitching moment obtained on a fighter configuration in 4T and 16T at transonic speeds.

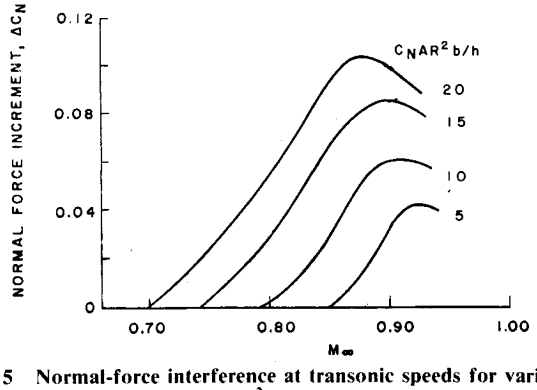

Fig. 15 Normal-force interference at transonic speeds for variation in the empirical parameter, $C_N \mathcal{R}^2 b/h$.

Summary

1) Lift, downwash, and blockage interferences have been isolated from other variables such as tunnel flow quality, "effective" Reynolds number, and model distortion under load, which can be present in comparative data.

2) The lift interference on a high-aspect-ratio transport configuration (ONERA calibration body) was found to be related to $C_N b/h$. The lift interference is highly nonlinear in C_N at transonic speeds, and its magnitude can approach 10% for typical model sizes and cruise lift coefficients. Downwash interference on the ONERA configuration appears to be equally pronounced and to conform generally to the classical parameter, $\bar{X} C_N S/h^3$.

3) Families of curves are presented which can be used to provide a measure of lift or pitching-moment interference for

high-aspect-ratio configurations. To minimize lift and pitching-moment interference for high-aspect-ratio configurations of the ONERA type, the model span to tunnel span ratio should be maintained at 0.2 or less at high transonic speeds and higher normal-force coefficients. Larger model span to tunnel height ratios are permissible for subsonic speeds and lower normal-force coefficients.

4) Fighter and lifting body configurations ($AR < 4$) are not nearly as sensitive to wall interference when tested at conventional model to tunnel size ratios. An empirical dependence of lift interference on AR^2 is suggested to reasonably account for the differing nature of the flowfields and possibly the effects of three-dimensional flow alleviation.

Acknowledgments

The research reported herein was performed by the Arnold Engineering Development Center, air Force Systems Command. Analysis for this research was done by personnel of ARO, Inc., a Sverdrup Corporation Company, operating contractor for the AEDC. Further reproduction is authorized to satisfy needs of the U.S. Government.

References

[1] Binion, T. W., "Tests of the ONERA Calibration Models in Three Transonic Wind Tunnels" Arnold Air Force Station, Tenn., AEDC-TR-76-133, Nov. 1976.

[2] Pate, S. R. and Schueler, C. J., "Radiated Aerodynamic Noise Effects on Boundary-Layer Transition in Supersonic and Hypersonic Wind Tunnels," *AIAA Journal*, Vol. 7, March 1969, pp. 450-457.

[3] Dougherty, N. S. and Steinle, F. W., "Transition Reynolds Number Comparisons in Several Major Transonic Wind Tunnels," AIAA Paper 74-627, AIAA 8th Aerodynamic Testing Conference, Bethesda, Md., July 1974.

[4] Mokry, M. and Galway, R. D., "Analysis of Wall Interference Effects on ONERA Calibration Models in the NAE 5 ft × 5 ft Wind Tunnel," National Research Council, Aero Rept. LR 594, March 1977.

[5] Vaucheret, X., Bazin, M., and Armand, C., "Comparison of Two and Three Dimensional Transonic Tests Made in Various Large Wind Tunnels," National Technical Information Service, Translation ADA021348, Feb. 1976.

[6] Poisson-Quinton and Vaucheret, X., "Prediction of Aerodynamic Characteristics of an Aircraft from a Correlation of Models Tested in Various Large Transonic Tunnels," presented at the AGARD Flight Mechanics Panel Specialists Meeting on Aricraft Performance and Predictions, Paris, Oct. 13, 1977.

[7] Couch, L. M. and Brooks, C. W., "Effect of Blockage Ratio on Drag and Pressure Distributions for Bodies of Revolution at Transonic Speeds," NASA TND 7731, Nov. 1973; also AIAA Paper 72-1008, presented at the 7th Aerodynamic Testing Conference, Palo Alto, Calif., Sept. 1972.

[8] Kraft, E. M. and Lo, C. F., "A General Solution for Lift Interference in Rectangular Ventilated Wind Tunnels," AIAA Paper 73-209, AIAA 11th Aerospace Sciences Meeting, Washington, D.C., Jan. 1973.